ELSEVIER

Chemical Engineering Journal 140 (2008) 497–508

Chemical Engineering Journal

www.elsevier.com/locate/cej

An innovative bed temperature-oriented modeling and robust control of a circulating fluidized bed combustor

Aboozar Hadavand [a,*], Ali Akbar Jalali [a], Parviz Famouri [b]

[a] *Department of Electrical Engineering, Iran University of Science and Technology, Elm-o-Sanat street, Narmak, Tehran 16846, Iran*
[b] *Lane Department of Computer Science and Electrical Engineering, West Virginia University, Morgantown, WV 26506, USA*

Received 12 October 2007; received in revised form 8 November 2007; accepted 26 November 2007

Abstract

Circulating fluidized bed (CFB) combustion systems are increasingly used as superior coal burning systems in power generation due to their higher efficiency and lower emissions. However, because of their non-linearity and complex behavior, it is difficult to build a comprehensive model that incorporates all the system dynamics. In this paper, a mathematical model of the circulating fluidized bed combustion system based on mass and energy conservation equations was successfully extracted. Using these correlations, a state space dynamical model oriented to bed temperature has been obtained based on subspace method. Bed temperature, which influences boiler overall efficiency and the rate of pollutants emission, is one of the most significant parameters in the operation of these types of systems. Having dynamic and parametric uncertainties in the model, a robust control algorithm based on linear matrix inequalities (LMI) have been applied to control the bed temperature by input parameters, i.e. coal feed rate and fluidization velocity. The controller proposed properly sets the temperature to our desired range with a minimum tracking error and minimizes the sensitivity of the closed-loop system to disturbances caused by uncertainties such as change in feeding coal, while the settling time of the system is significantly decreased.

Keywords: Circulating fluidized bed (CFB); Bed temperature; Subspace identification; Robust control; Linear matrix inequalities (LMI)

1. Introduction

Today there is no doubt that fluidized bed combustion (FBC) systems are superior to all other combustion technologies in burning low quality coals, biomass and other waste fuels. Effective combustion with high system efficiency even for low-reactivity fuels is accessible with applying a proper control structure, and it is possible for these kinds of systems to achieve combustion efficiency of up to 99.5% [1]. On the other hand, combustion of coal with high sulfur content, when strict requirements for environmental protection have to be satisfied, is feasible only in FBC systems. These systems are noticeably suitable for steam generation purposes in high capacities in power plants as they can satisfactorily respond to variations in load demands. They can handle load changes of up to 4% per minute without any problems [2].

"Fluidization" refers to the condition in which solid materials are given free-flowing, fluid-like behavior. As gas is passed upward through a bed of solid particles, the flow of gas produces forces which tend to separate the particles from one another [3]. In a typical FBC which uses air as the fluid (atmospheric fluidized bed), fine particles of coal are injected to the bed by air. Air nozzles are located in the bottom and the combustion chamber wall. Injected coal particles first produce volatiles over a relatively short period of time. The char particles which remain after complete devolatilization burn for a relatively long period of time [4]. With an increase in air velocity, large amounts of particles are carried out of the bed with the air. Entrained particles must be collected by the cyclone (which includes standpipe section) and returned to the bed. These types of systems are generally called circulating fluidized beds (CFBs). CFBs use a higher fluidizing velocity, so the particles are constantly held in the flue gases, and pass through the main combustion chamber and into the cyclone. Fig. 1 shows a simplified diagram of a circulating fluidized bed combustor.

The fluidized bed is not yet a fully understood system and its dynamics is very complex because of its chaotic nature, non-

* Corresponding author. Tel.: +98 21 22072701; fax: +98 21 22080207.
E-mail address: a_hadavand@ee.iust.ac.ir (A. Hadavand).

1385-8947/$ – see front matter © 2007 Elsevier B.V. All rights reserved.
doi:10.1016/j.cej.2007.11.032

Nomenclature

A	surface area (m^2)
A'	constant in Eq. (14)
c	specific heat capacity (kJ/kg K)
C_g	oxygen concentration in the free stream (kPa)
d	diameter (m)
D_b	bed diameter (m)
D_g	molecular diffusivity of oxygen (m^2/s)
E	activation energy (kJ/kmol)
G	average circulation rate (kg/m^2 s)
h	total heat transfer coefficient (W/m^2 K)
h_m	mass transfer coefficient (kg/m^2 kPa s)
H	bed height (m)
H_c	combustion heat (kJ/kg)
H_v	heat produced by combustion of volatiles (kJ/kg)
k_a	attrition constant
k_c	char reaction rate coefficient (kg/m^2 kPa s)
k_g	thermal conductivity of the gas (W/m K)
m	mass (kg)
M	bed mass (kg)
P	bed pressure (kPa)
P	heat generated per unit time (kJ/s)
P_a	power delivered to heat the air mass flow from the inlet temperature to the bed temperature (kJ/s)
P_b	heat generated per unit time by the burning of char (kJ/s)
P_{bw}	heat transported from the bed to wall heat exchangers (kJ/K)
q	volume flow rate (m^3/s)
Q	heat per unit time (kJ/s)
R	universal gas constant (kPa m^3/kmol K)
Re	Reynolds number
Sc	Schmidt number
Sh	Sherwood number
T	temperature (K)
T_m	mean temperature of the diffusion layer around the carbon particle (K)
u_s	slip velocity (m/s)
U	fluidization velocity (m/s)
V	volume (m^3)
x_v	fraction of volatile matters

Greek letters

ε	bed voidage
ζ	particle porosity
μ	viscosity of gas (kg/m s)
ρ	density (kg/m^3)
ρ_s	suspension density of the bed (kg/m^3)
φ	combustion reaction mechanism factor
ω_a	attrition rate (kg/s)
ω_b	char burning rate (kg/s)
ω_c	char flow rate (kg/s)
ω_f	burning rate of fine particles (kg/s)
ω_i	coal feed rate (kg/s)

Subscripts

b	bed
c	char
c	convective
f	fines
g	gas
m	number of inlet flows
mf	minimum fluidization
p	particle
r	number of outlet flows
s	number of heat sources and consumptions
s	solids
v	volatiles
w	wall heat exchangers

linearity, and number of immeasurable unknown parameters [5]. Obviously, the conditions under which the combustion of coal particles in a fluidized bed takes place are significantly different from the combustion conditions in other types of boilers. Research on these combustion processes requires an understanding of coal combustion process in fluidized beds.

The dynamics of multi-phase flow and process characteristics of circulating fluidized bed boilers have been discussed by many authors [5–12]. The goal of these research projects has been the mathematical modeling of gas/solid flow in different parts of the fluidized bed; however, they are mainly focused on cold systems and the particles flow dynamics. Hence, bed temperature and its effects on system dynamics are ignored. Modeling and control of combustion process when the system works in real conditions have been studied by [13–18]. Bed temperature, which influences steam temperature and boiler overall efficiency, is one of the most significant parameters in the operation of these types of systems. Many other reasons for controlling bed temperature

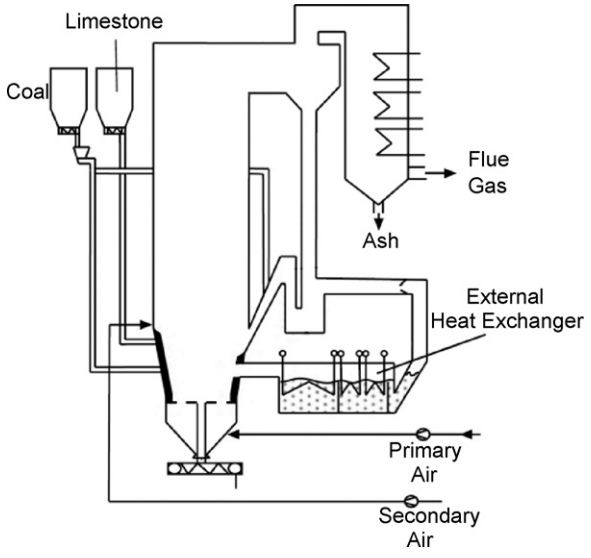

Fig. 1. Schematic diagram of a circulating fluidized bed combustion system.

includes better sulfur capture and less gaseous pollutants emission included in the exhaust gas. Bed temperature also has a direct effect on system internal parameters which was studied by Cue and Chaouki [19]. Therefore, it must be bounded in a certain range; it means that it should be high enough so that the fuel particles burn completely, and should be low enough to prevent combustion chamber's walls and heat exchanger's melting and also ash agglomeration. From this place, modeling and control of CFB combustion systems in operational conditions is one of the most challenging problems in chemical reactors engineering.

In this project a well-suited mathematical model of the mass and heat transfer processes in a circulating fluidized bed combustion system based on mass and energy conservation equations is obtained. Using these correlations, a state space dynamical model of bed temperature has been extracted based on subspace method. Having dynamic and parametric uncertainties in the model, a robust control algorithm based on linear matrix inequalities (LMI) have been applied to control the bed temperature by input parameters, i.e. coal feed rate and fluidization velocity. The results are shown for open- and closed-loop systems. To test the validity of the proposed robust controller, the effect of change in fuel particles on the closed-loop system's response is observed. Finally, the effect of bed temperature on the combustion process is discussed.

2. Combustion process mathematical model of a CFB

Every process is determined with its physical and chemical nature that expresses its mass and energy bounds. Investigation of any typical process leads to the development of its mathematical model. Mathematical models are abstractions of real processes. They give a possibility to characterize behavior of processes if their inputs are known. By the construction of mathematical models it is possible to extract dynamical models which are important for control purposes.

To obtain a precise and practical mathematical model of bed temperature in a CFB unit, one should apply theoretical relations based on mass and energy conservation equations along with correlations based on well-conducted experimental approaches. Mass balances for lumped parameter processes in an unsteady-state are given by the law of mass conservation and can be expressed as

$$\frac{d(\rho V)}{dt} = \sum_{i=1}^{m} \rho_i q_i - \sum_{j=1}^{r} \rho_j q_j \tag{1}$$

where ρ is the density, V the volume, q the volume flow rate, m the number of inlet flows, and r is the number of outlet flows. Energy balances follow the general law of energy conservation and can be written as

$$\frac{d(\rho VcT)}{dt} = \sum_{i=1}^{m} \rho_i q_i c_i T_i - \sum_{j=1}^{r} \rho_j q_j c_j T_j + \sum_{l=1}^{s} Q_l \tag{2}$$

in which c is the specific heat capacity, T the temperature, Q heat transfer per unit time, and s is the number of heat sources and consumptions as well as heat brought in and taken away not in inlet and outlet streams.

Thus, the char mass conservation equation in a circulating fluidized bed combustion system which incorporates char flow rate and also char burning and attrition rates is given by

$$\frac{d}{dt} m_c = \omega_c - \omega_b - \omega_a. \tag{3}$$

here m_c is the char mass, ω_c is the char flow rate and is a fraction of the coal feed rate, ω_b is the char burning rate, and ω_a is the attrition rate of char particles. In the next two sections, the equations governing char burning and attrition processes will be discussed. The energy conservation equation in a CFB is as follows

$$(c_s M_s + c_c m_c)\frac{d}{dt} T_b = P_b + P_v + P_f - P_{bw} - P_a \tag{4}$$

where, $c_s M_s$ and $c_c m_c$ are heat capacities related to solid and char particles, respectively, and P_b, P_v, and P_f are the heat generated per unit time by the burning of char, volatiles and fine particles. Here P_{bw} is the heat transported from the bed to wall heat exchangers and P_a is the power delivered to heat the air mass flow from the inlet temperature to the bed temperature. Power generated from the burning of char, P_b is as follows

$$P_b = \omega_b H_c \tag{5}$$

in which H_c is the combustion heat. The term P_v can be expressed by

$$P_v = \omega_i x_v H_v \tag{6}$$

where H_v is the heat produced by combustion of volatiles. Energy delivered from the combustion of fines which relates to the burning rate of fine particles, ω_f, is given by

$$P_f = \omega_f H_c. \tag{7}$$

These fine particles are mainly produced from parent coal and attrition of char. The term P_{bw} which is the heat transported from the high temperature bed materials to the wall heat exchangers is computed by the following correlation:

$$P_{bw} = hA_w(T_b - T_w) \tag{8}$$

where T_w is the wall heat exchangers temperature and A_w is their surface area. h is the total heat transfer coefficient which will be completely discussed in Section 2.3.

To predict properties, or for the mathematical modeling of combustion process in CFB boilers, it is necessary to know the burning, attrition, and heat transfer processes.

2.1. Char particles burning

Char is a combustible matter left over after devolatilization of coal particles. Char formed after the volatile evolution has an inner structure which is very different from that of the initial coal. Studying the char combustion process is essential because of its effects on combustion hydrodynamics. The burning rate of char particles has a significant influence on the combustion process; it determines, e.g. the carbon hold up in a fluidized bed which

affects the carbon loss by attrition and elutriation and thus the combustion efficiency [4]. Understanding the char combustion process, gives us the ability to have a comprehensive perception of modeling and controlling the bed temperature in a fluidized bed and the ability to predict the system's combustion efficiency. Three different models have been introduced for char burning, which are

- unreacting shrinking core model,
- reacting core model, and
- progressive conversion model

which differ in where the combustion takes place (inner or outer surface of the particle) and what order of oxidation reaction is assumed [1]. The combustion of char is a high temperature oxidation of carbon to carbon dioxide. The reaction is described as follows:

$$C + \left(\frac{1}{\varphi}\right) O_2 \rightarrow \left(2 - \frac{2}{\varphi}\right) CO + \left(\frac{2}{\varphi - 1}\right) CO_2$$

where φ is the mechanism factor and is equal to 1 for the first model and 2 for the second and third models. In a circulating fluidized bed, the abrasion of ash layer by the high gas–solid relative velocity continuously takes places on the char surface. Thus, the shrinking unreacted core model is considered in most studies especially in studying the industrial and large scale systems [20]. As it can be seen, the main product of char combustion reaction in the shrinking core model is CO_2 instead of CO.

In modeling the bed temperature, some assumptions in char combustion process should be considered: we assume that the solids are perfectly mixed, their distribution is independent of operating conditions, the coal combustion model is described by the so-called shrinking core model and the reaction kinetics is of order one. Also the temperature field is assumed to be homogeneous, due to intense inert material particle mixing, and the intense heat transfer between particles and between gas and particles.

Combustion processes are similar in circulating or bubbling fluidized beds, but the burning rate of char are different in these beds. The burning rate of char in circulating fluidized beds is higher than that in bubbling beds due to higher mass transfer rate [21]. The burning rate of char particles in a circulating fluidized bed burning in the shrinking core regime ($\varphi = 1$) is as follows [22]

$$\omega_b = \frac{C_g}{1/h_m + 1/k_c} A_c \tag{9}$$

where K_c is the char reaction rate coefficient, C_g is the oxygen concentration in the free stream, A_c is the surface area of a char particle, and h_m is given by

$$h_m = \frac{12 Sh \varphi D_g}{d_c R T_m} \tag{10}$$

here D_g is molecular diffusivity of oxygen, d_c is carbon particle diameter, T_m the mean temperature of the diffusion layer around the carbon particle, Sh is Sherwood number, and R is the universal gas constant which is equal to 8.315 kPa m^3/(kmol K).

Calculating the Sherwood number Sh has been studied by Souza-Santos [23]. The approximation of the Sherwood number for circulating fluidized beds is given by

$$Sh = 2\varepsilon + 0.69 \left(\frac{Re}{\varepsilon}\right)^{0.5} Sc^{0.33} \tag{11}$$

where ε is bed voidage, and Re, Sc are Reynolds and Schmidt numbers, respectively, which can be calculated as follows

$$Re = \frac{u_s d_c \rho_g}{\mu_g}, \tag{12}$$

$$Sc = \frac{\mu_g}{\rho_g D_g}. \tag{13}$$

here u_s is slip velocity which can be found as, $u_s = U/\varepsilon - G_s/(1-\varepsilon)\rho_c$, where G_s is the average solids circulation rate. Mean temperature of diffusion layer around particle, T_m can be calculated as $(T_b + T_s)/2$, in which, T_b is bed temperature and T_s is particle temperature. Brem [4] concluded from experimental simulations that one could easily take the char particles temperature equal to the bed temperature. It is characteristics of chemical reactions that their rate coefficients depend strongly in a nonlinear way on the temperature [24]. Char reaction rate coefficient, k_c is generally given by [2]

$$k_c = A' \exp\left(\frac{-E}{RT_s}\right) \tag{14}$$

in which the activation energy and the coefficient, A' vary with the characteristics of coal and its chemical composition [25] and are obtained by empirical studies. The diffusivity coefficient D_g depends on the particle porosity, temperature, pressure and its concentration. The following simple correlation can be used to compute the average diffusion coefficient of oxygen in a fluidized bed [26]

$$D_g = 8.677 \times 10^{-8} \frac{T_b^{1.75}}{P} \zeta^2 \tag{15}$$

where ζ is particle porosity.

2.2. Char particles attrition

During char combustion process, due to collisions with inert bed particles, abrasion of char particles takes place and small particles of char separate from the main particle. This process, called attrition, depends on the coal type and may produce a significant amount of very small combustible particles [1].

The attrition rate of char particles in a bubbling fluidized bed (BFB) has been obtained by Donsi et al. [27]. The mass flow rate of char consumed by attrition in a circulating fluidized bed, ω_a is proportional to the char mass, mean slip velocity between the char particle and the fine bed solids and a determined constant. Halder [28] presented the following correlation for calculating the attrition rate in a CFB:

$$\omega_a = k_a \left(U_c - \frac{G_s}{\rho_b}\right) \frac{m_c}{d_c} \tag{16}$$

where, ρ_b is the average bed density of the bed, U_c is the char velocity, and k_a is the attrition constant. The attrition constant is independent of the fluidization regimes [28] and depends only on the coal type. Attrition constants of different coal types have been collected by Brem [4].

Talmor and Benenati [29] proposed the average circulation rate of particles as

$$G_s = 785\,(U - U_{mf})\exp(-6630 d_c) \tag{17}$$

where U_{mf} is the minimum fluidization velocity. Therefore, the difference between the actual fluidization velocity and the minimum value has a strong influence on the circulation rate of particles in the bed. The bed density, ρ_b, refers to the average density of the bed above the combustion zone and is determined from the pressure drop measured across the upper section of the riser [2] or it can be found from the following simple correlation

$$\rho_b = \frac{M}{A_b H} \tag{18}$$

in which, M is the total mass of the bed, A_b is the cross-section area of the bed, and H is the bed height. The char velocity can be found as

$$U_c = \frac{G_s}{(1-\varepsilon)\rho_c} \tag{19}$$

where ρ_c is the char density.

2.3. Heat transfer process

Heat transfer plays a significant role in the hydrodynamics of a CFB combustion unit where the primary objective is to transfer heat from the high temperature bed to produce steam for turbines. The magnitude of the heat transfer and location of heat transfer surfaces of a boiler greatly influence its thermal efficiency [2]. In a fluidized bed combustor, heat is transported by circulating suspended solid particles to the heat transfer surfaces which are commonly vertical surfaces in the form of membrane walls [30]. Heat transfer from a fluidized bed to membrane walls is generally seen to consist of three components: particle convection, radiation convection and gas convection among which the latter one is usually disregarded due to the lower density of the gas compared to the solids [31]. Thermal conduction is also neglected when considering heat transfer in CFB combustion systems [32].

Many different correlations have been proposed for modeling the heat transfer process in fluidized beds [33–36]. Werdmann and Werther [33] have extracted the following correlation for the convective heat transfer coefficient

$$h_c = 7.46 \times 10^{-4} \left(\frac{k_g}{d_p}\right) \rho_s^{0.562} \left(\frac{D_b \rho_g u_g}{\mu_g}\right)^{0.757} \tag{20}$$

where ρ_s is suspension density of the bed and k_g is the thermal conductivity of the gas. Suspension density seems to be the most significant factor influencing the heat transfer. Correlation (20) must be added to the radiative coefficient to obtain the overall heat transfer coefficient. By neglecting the heat radiation and convection in the dilute phase, a simpler empirical correlation for the overall heat transfer to the water wall of a CFB presented by Dutta and Basu [37] is given by

$$h\,(\mathrm{W/m^2\,K}) = 5\rho_s^{0.391} T_b^{0.408} \tag{21}$$

3. Bed temperature dynamic model of a CFB

In the past section, the mathematical model of the bed temperature in the riser of a circulating fluidized bed combustion system was obtained. These correlations could be collected as a set of nonlinear ordinary differential equations. The next step is to estimate a dynamic model based on the mathematical model extracted for optimization and control purposes. Optimization in the combustion system results in maximizing thermal efficiency and minimizing pollutant emissions and operating costs. The choice of combustion temperature is an important issue in the design of fluidized bed boilers. Circulating fluidized bed boilers typically operate in the range of 1100–1200 K. The bed temperature (combustion temperature) should be controlled for the following reasons: (1) to improve combustion efficiency which is dependent on the bed temperature, (2) to have the optimal sulfur capture, (3) to prevent ash agglomeration at the bottom of the combustor chamber, (4) to prevent combustion chamber's walls and heat exchangers melting, (5) to prevent vaporizing alkali metals from the coal which causes fouling (these metals would not vapor at low temperatures), and (6) to lower pollutants emission such as CO and NO_x.

The combustion efficiency generally increases with the bed temperature because the carbon fines burn faster at high temperatures and a higher temperature may help reduce the burnout time and hence the combustible loss. The effect of temperature is especially important for less reactive fuel particles such as anthracite or petroleum coke. High combustion temperature is beneficial especially for low volatile, less reactive fuels [2].

Cui and Chaouki [19] studied the effects of bed temperature on the local two-phase flow structure in a pilot scale fluidized bed of the FCC particles with bed temperatures ranging from 25 °C to 420 °C, covering both the bubbling and turbulent fluidization regimes. However, the temperature range considered is not realistic, but easily shows the effect of temperature on system internal parameters. The results show that fluidization is enhanced and fluctuations of the local two-phase flow structure become more intense with increasing bed temperature. At constant superficial gas velocities, the averaged local particle concentration, the dense phase fraction and particle concentration in the dense phase decrease with increasing bed temperature.

Bed temperature also affects the pollutants emissions. To study the effect of combustion temperature on NO_x emission, its production sources must be understood. The major source of NO_x production from nitrogen-bearing fuels such as certain coals is the conversion of fuel bound nitrogen to NO_x (fuel NO_x). During combustion, the nitrogen bound in the fuel is released as a free radical and ultimately forms free N_2 or NO. Fuel NO_x can contribute as much as 80% when combusting coal. A second source of NO_x formation is the oxidation of nitrogen in the combustion air (thermal NO_x). Thermal NO_x increases with rising temperature, nitrogen concentration in the flame, oxygen

concentration and gas residence time [38]. In low temperatures very little atmospheric nitrogen is converted to NO_x. Brem [4] studied the effects of bed temperature and concluded that NO emission increases linearly as the bed temperature increases. This increase is caused by the increase of volatile production and an enhancement of the ammonia oxidation rate to NO_x at higher temperatures. The effect of temperature on CO emission is completely different from that we have for NO_x. Brem [4] showed both theoretically and empirically that CO emission decreases linearly with the raise in the bed temperature. What is important here is, that both pollutants can be reduced if the plant is operated correctly and the bed temperature is well controlled.

Very high temperatures may also result in ash agglomeration at the bottom of the furnace causing problems such as flooding of the cyclone. This prevents the solids flow through the loop seal and leads to complete choking [2].

Bed temperature control is commonly accomplished by auxiliary fuel flow control and the primary airflow [15]. In this study the control scheme is to keep the bed temperature in a desirable certain range through the coal feed rate and fluidization velocity. These two parameters highly influence the combustion process. When the feed rate is increased, first the feed fraction (reactant) will increase. This increased fraction leads to a higher rate of reaction, and consequently the heat production will increase. Likewise, the fluidization velocity affects the process of mass transfer between fuel particles and the bed, the rate of volatiles released, and the char particles attrition [1]. It also has an indirect effect on the heat transfer through the change in the suspension density; suspension density will become more with decreasing fluidizing velocity.

Thus, the process is characterized via three parameters: coal feed rate and fluidization velocity (as inputs), and bed temperature (as output). Now, one could extract a multi-input and single-output (MISO) model, which tells us how the input variables affect the output. The selection of good excitation signals is an important step in the design of the experiment. In this study, generalized multiple-level noise (GMN), which is a multiple-level generalization of generalized binary noise (GBN) is used as the model input and then the output (bed temperature) is measured. This method involves a generalized stochastic distribution of the switching moments, which allows manipulation of the frequency spectrum of the input signal, such that most energy is concentrated in the lower frequencies [39]. The GMN concept indeed gives much better identification results than conventional concepts especially for processes with delays. Also unlike a low-pass pseudo-random binary sequence (PRBS) signal, the spectrum of a low-pass GMN signal does not have dips at some frequencies. Another advantage with GMN is that the signal length is flexible [40]. The GMN signal is generated as the excitation signal at 15 levels for u_1 (coal feed rate) and at 23 levels for u_2 (fluidization velocity) to cover all the operating points. The average switching time between these levels is selected as 6 samples and 2000 samples are used for identification. Fig. 2 shows the input and output data collected for identification of the process. In order to have a more realistic simulation of the CFB boiler and to be able to tune the control parameters reliably for real applications, the important parameters to specify the mathematical equations related to the process and coal particles are given in Tables 1 and 2. These set of parameters are from a pilot boiler by Babcock & Wilcox Co. in [23] which uses petroleum coke as input coal.

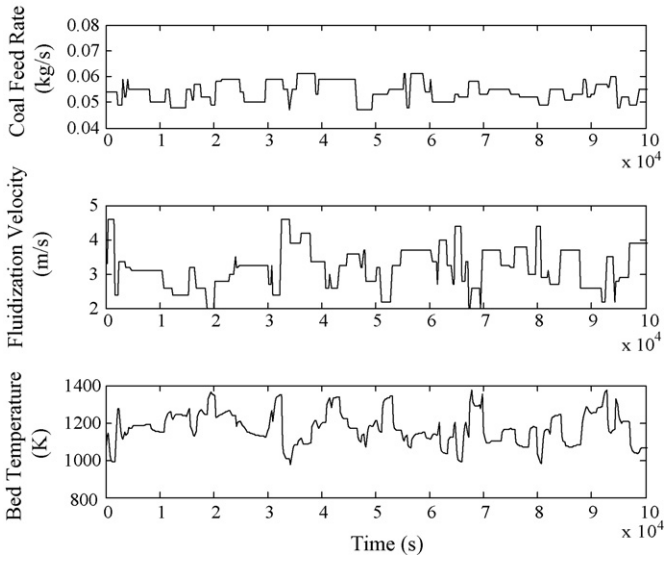

Fig. 2. GMN input and output signals for identification of the CFB combustion system.

Table 1
Process parameters (Babcock & Wilcox 80 firebrick)

Plant parameters	Nominal value
Bed height (m)	0.8
Bed diameter (m)	1.2
Average reactor internal pressure (kPa)	102
Injected air temperature (K)	305

There are many methods to build a model from the generated random input–output data. To choose a model structure that is suitable for identification one should refer to the system properties. A more exact model leads to better error variances between the predicted data and real data. In this study the subspace method is used to build a linear state space model from the data. If the process is controlled and the operating range is small, a linear process model may be an adequate approximation of reality. Further, a linear model is more proper when designing model-based controllers such as robust control algorithms. The subspace method is found to be the best choice among the others from the viewpoint of data fit and the order of the model. The following section explains the basic idea behind the method.

Table 2
Nominal values of model parameters for petroleum coke

Model parameters	Nominal value
Char particle diameter (mm)	1.5
Heat value of the feed coal (kJ/kg)	32,500
Volatile content of the feed coal (%)	28
E/R (K)	9,058
A' (kg/m^2 s kPa)	1.97
k_a	1.5×10^{-7}

Consider a representation of a discrete-time linear time-invariant (LTI) system of the form:

$$\begin{aligned} x(t+1) &= Ax(t) + Bu(t) + w(t) \\ y(t) &= Cx(t) + Du(t) + v(t) \end{aligned} \tag{22}$$

where y is the output vector, u the input vector, x the state vector, w, v the noise terms, and A, B, C, and D are to be estimated system matrices. Let us define the extended observability matrix as

$$O_r = [C,\ CA,\ CA^2, \ldots,\ CA^{n-1}]^T \tag{23}$$

where n is the dimension of matrix A. For any invertible matrix T, one can rewrite the system as

$$\begin{aligned} \tilde{x}(t+1) &= T^{-1}AT\tilde{x}(t) + T^{-1}Bu(t) + \tilde{w}(t) \\ y(t) &= CT\tilde{x}(t) + Du(t) + v(t) \end{aligned} \tag{24}$$

The extended observability matrix, O_r, is also changed to $\tilde{O}_r = O_r T$. By the assumption that this basis change does not affect the original system dynamic matrix [41], the defined system Eq. (24) leads to

$$\begin{aligned} y(t+k) = {} & CA^k x(t) + CA^{k-1}Bu(t) + \cdots + CBu(t+k-1) \\ & + CA^{k-1}w(t) + CA^{k-2}w(t+1) \\ & + \cdots + Cw(t+k-1) + v(t+k) \end{aligned} \tag{25}$$

If we rewrite them in a vector form, we arrive at

$$Y_r(t) = O_r x(t) + S_r U_r(t) + V(t) \tag{26}$$

where

$$S_r = \begin{pmatrix} D & \cdots & 0 \\ CB & \cdots & 0 \\ \vdots & \ddots & \vdots \\ CA^{r-2}B & \cdots & D \end{pmatrix} \tag{27}$$

The basic concept of subspace identification method is to calculate A, B, C and D matrices using least squares by finding the extended observability matrix. This is performed by eliminating the input and noise terms in Eq. (26) using known input and output matrices. The least squares estimate of system dynamic matrices is given by [42]

$$\begin{aligned} \begin{pmatrix} A & B \\ C & D \end{pmatrix} = {} & \left(\sum_{t=0}^{n-1} \begin{pmatrix} \tilde{x}(t+1) \\ y(t) \end{pmatrix} (\tilde{x}^T(t)\, u^T(t)) \right) \\ & \times \left(\sum_{t=0}^{n-1} \begin{pmatrix} \tilde{x}(t) \\ u(t) \end{pmatrix} (\tilde{x}^T(t)\, u^T(t)) \right)^{-1} \end{aligned} \tag{28}$$

This class of approaches is called the direct N4SID method. The estimated linear model of the circulating fluidized bed system is calculated using N4SID method, which is of order 3. The order of the model should be a trade-off between the complexity of the model and its validity. For industrial processes, in many instances, low order models will suffice, especially when the process is kept in a certain operating point.

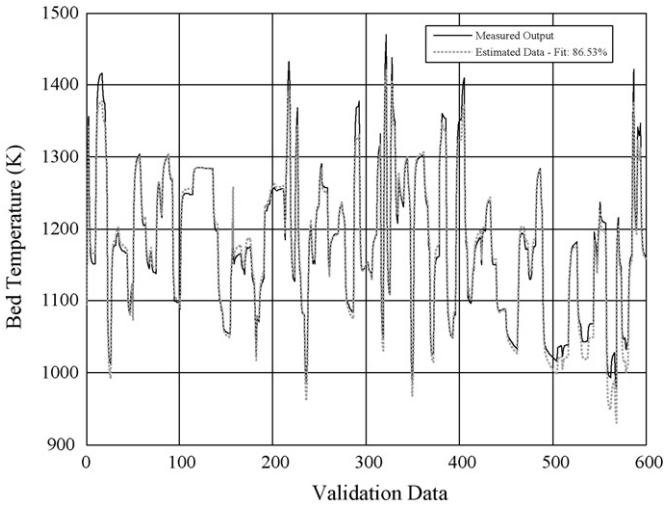

Fig. 3. Comparison between the data obtained from the real system and the estimated data.

A model is not useful until its validity has been tested and established. The model is usually identified by minimizing the error between process data and model prediction. A criterion should be defined which indicates how good the model fit is. For a process operating around a steady-state value, one could use:

$$\text{Fit} = 100 \times \left(1 - \frac{\text{norm}(y - \hat{y})}{\text{norm}(y - \bar{y})}\right) = 86.5\% \tag{29}$$

in which $\hat{y}$ is the model prediction and $\bar{y}$ the mean or average value of the data series [43]. A comparison between the measured data and the estimated model data is shown in Fig. 3. The results show that the estimated data 86.5% fits the real system data.

Besides comparing models in terms of the prediction variances that they produce, the models can be simulated with a given input and then compared as to how well they describe the corresponding measured output [44]. The results are shown for

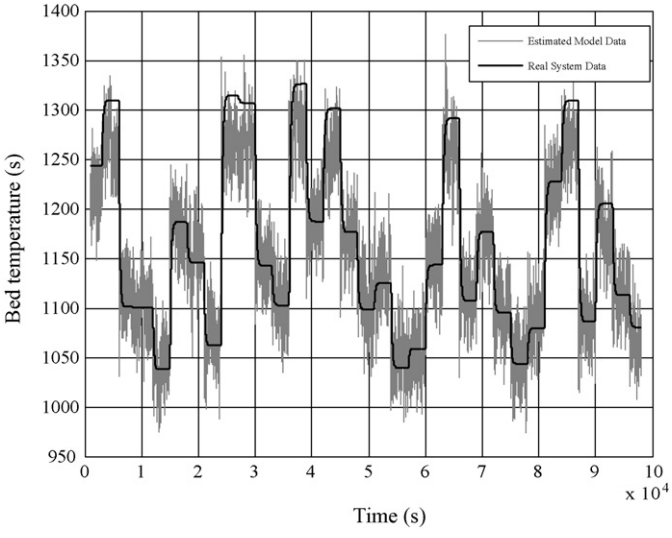

Fig. 4. Outputs of the real system and the estimated model to the random level step changes in fluidization velocity.

the real system's and estimated model's outputs to the random level step changes in fluidization velocity in Fig. 4.

As it can be seen, the model proposed agrees reasonably well with the experimental results. The advantage of this model is that it is not solely based on experimental data gathered from a specific plant so that the controller designed based on the model could not be used on other plants. This is the value of modeling based on mathematical correlations; one could easily change the model parameters from plant to plant to build a new dynamic model and controller. Now, we can continue the controller design procedure with of the third-order state space model. Organization of the paper follows the requirement of presentation of the H_∞ control algorithms that take into account changes of static and dynamic properties of process. In this paper, LMI optimization approach will be used to design the reliable H_∞ control for the uncertain boiler. The next section is devoted to LMI techniques to robustly control the bed temperature in a circulating fluidized bed combustion system.

4. Control of bed temperature in a CFB

Chaotic nature of fluidized bed combustion systems together with variation in their parameters such as time-variant char particle diameter during the combustion process and changing in the quality of the feed coal [14] result in uncertainties in the model obtained. Also, it should be considered that the theoretical and empirical correlations used for process identification and modeling may not be precise causing deviations from the real system model. On the other hand, presences of unknown variables, which affect the system performance along with inaccuracies in measurements, make the controlling of the system hard. Therefore, the first possibility is to design a robust controller based on the linear state space model and then to apply it on the nonlinear mathematical model. In practical studies, it is important when designing a controller to guarantee a good closed-loop stability and performance for all possible operating conditions of the plant. So in the case that the values of the plant parameters estimated through experiments vary with the change of operating conditions, it is unavoidable to incorporate the parameter variation into the control design [45].

The design of robust controllers using Linear matrix inequalities (LMIs) has long been considered as one of the most important solutions in the control of these types of systems [46–50]. LMIs have emerged as a powerful formulation and design technique for a variety of linear control problems [51]. Boosted by the availability of fast LMI solvers, research in robust control has experienced a significant paradigm shift. The basic idea of the LMI method in control is to approximate a given control problem via an optimization problem with linear objective and so-called LMI constraints. The LMI method leads to an efficient numerical solution and is particularly suited to problems with uncertain data and multiple specifications.

4.1. Linear matrix inequalities (LMI) in control

This section gives a formal statement of the LMI control problem and defines the relevant notation. Consider the state

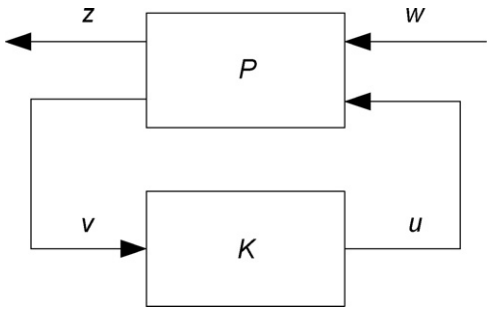

Fig. 5. Representation of the closed-loop system.

space representation of the LTI system depicted in Fig. 5 as

$$\begin{cases} \dot{x} = Ax + B_w w + Bu \\ z = C_z x + D_{zw} w + D_z u \\ y = Cx + D_w w + Du \end{cases} \tag{30}$$

where w is the disturbance signal, and z is a vector of output signals related to the performance of the control system. In a realistic design problem one is usually not just confronted with a single-objective problem but one has to render various objectives satisfied. For example the control objective could be to weaken the effect of disturbances and modeling uncertainties as small as possible, to reduce the control effort, and to bound the settling time of the closed-loop system to some extent. Thus, in this case, the performance vector z contains the output y and inputs u_1 and u_2 and the specification related to settling time bounds.

The controller K of the form

$$\begin{cases} \dot{\zeta} = A_K \zeta + B_K y \\ u = C_K \zeta + D_K y \end{cases} \tag{31}$$

must meet the specifications on the closed-loop behavior. These specifications are formulated relative to some closed-loop transfer function of the form

$$T_j = L_j T R_j \tag{32}$$

in which T denotes the closed-loop transfer functions from w to z, and the matrices L_j, R_j select the appropriate input/output (I/O) channels or channel combinations. Note that $T_j(s)$ is the transfer function from w_j to z_j such that

$$w = R_j w_j, \quad z_j = L_j z \tag{33}$$

with the plant P and controller K defined as above, the state space realization of the closed-loop system is given by [52]

$$T : \begin{cases} \dot{x}_{cl} = A_{cl} x_{cl} + B_{cl} w \\ z = C_{cl} x_{cl} + D_{cl} w \end{cases} \tag{34}$$

where

$$\left[\begin{array}{c|c} A_{cl} & B_{cl} \\ \hline C_{cl} & D_{cl} \end{array}\right] = \left[\begin{array}{cc|c} A + BD_K C & BC_K & B_w + BD_K D_w \\ B_K C & A_K & B_K D_w \\ \hline C_z + D_z D_K C & D_z C_K & D_{zw} + D_z D_K D_w \end{array}\right]. \tag{35}$$

with

$$B_j = B_w R_j, \quad C_j = L_j C_z, \quad D_j = L_j D_{zw} R_j \qquad E_j = L_j D_z, \quad F_j = D_w R_j \tag{36}$$

$T_j(s) = L_j T(s) R_j$ admits the realization

$$\left[\begin{array}{c|c} A_{cl} & B_{cl,j} \\ \hline C_{cl,j} & D_{cl,j} \end{array}\right] := \left[\begin{array}{c|c} A_{cl} & B_{cl} R_j \\ \hline L_j C_{cl} & L_j D_{cl} R_j \end{array}\right] = \left[\begin{array}{cc|c} A + BD_K C & BC_K & B_j + BD_K F_j \\ B_K C & A_K & B_K F_j \\ \hline C_j + E_j D_K C & E_j C_K & D_j + E_j D_K F_j \end{array}\right] \tag{37}$$

Now we intend to capture all of the specifications and objectives in the LMI framework. If A_{cl} and x_{cl} denote the closed-loop state matrix and state vector, respectively, and if $V(x_{cl}) = x_{cl}^T P x_{cl}$ be the quadratic Lyapunov function with $P > 0$, the stability criterion of the system is to satisfy the following inequality

$$A_{cl}^T P + P A_{cl} < 0 \tag{38}$$

The LMI approach consists of expressing each control specification or objective as an additional constraint on closed-loop Lyapunov functions satisfying Eq. (38). As mentioned before, in the case of multiobjective control, we consider all the specifications on a generic closed-loop transfer function $T_j(s)$. The corresponding LMI constraints are therefore formulated in terms of the state–space matrices A_{cl}, $B_{cl,j}$, $C_{cl,j}$, $D_{cl,j}$, H_∞ norm of the T_j which is its largest gain across frequency in the singular value norm is smaller than γ and the matrix A_{cl} is stable if and only if there exists a symmetric matrix P with

$$\begin{pmatrix} A_{cl}^T P + P A_{cl} & P B_{cl,j} & C_{cl,j}^T \\ B_{cl,j}^T P & -\gamma I & D_{cl,j}^T \\ C_{cl,j} & D_{cl,j} & -\gamma I \end{pmatrix} < 0, \quad P > 0 \tag{39}$$

4.2. H_∞ Control of bed temperature in a CFB: an LMI approach

Many criteria based on time responses or frequency responses can be used to find the best controller settings in a control design procedure [53]. Some of them such as short settling time, small steady-state error, limited overshoot, and desirable gain and phase margins are the most important ones for us. Stability is a minimum requirement for the good performance of a control system. However, in most practical cases, a desirable controller must admit a well-damped and quick time response. A common method to guarantee a suitable transient response is to place the closed-loop system poles in the desired place. Pole assignment in convex regions of the left-half plane can also be expressed as LMI constraints on the Lyapunov matrix P. These LMI regions are any region R of the complex plane that can be defined as [54]:

$$R = \{z \in C : L + zM + \bar{z}M^T < 0\} \tag{40}$$

where $L = L^T$ and M are fixed real matrices. The matrix-valued function $f_D(z)$ which is called the characteristic function is given by

$$f_D(z) = L + zM + \bar{z}M^T \tag{41}$$

In the case that the LMI region is the half plane with $Re(Z) > -\alpha$, the characteristic function equals to

$$f_D(z) = z + \bar{z} + 2\alpha < 0 \tag{42}$$

In this paper, to have the settling time shorter than about 500 s, the values of matrices L, M are obtained to be $2 + i$ and 1, respectively. Having the specification and objectives defined, one could find the H_∞ robust controller for the bed temperature model. The controller obtained is of third-order, which is equal to the model order. The achieved H_∞ norm of the closed-loop system is found to be 1.88 in the iteration, which is admissible. It is the importance of good modeling and control. The H_∞ norms show that how well a system can reject the disturbances.

5. Results and discussion

The Bode plot of the complementary sensitivity matrix which is a measure of disturbance rejection of a system is shown for our state space model compared with an ill-conditioned model obtained from ARX algorithm is shown in Fig. 6.

The smaller the Bode plot peak, the more robust the closed-loop system would be. Fig. 7 illustrates the step response of the closed-loop system compared with the open-loop one. As it can be seen from the figure, the settling time of the closed-loop system has been highly improved which was one of our goals. The results are also shown for the response of the closed-loop system to a random level reference input in Fig. 8. In this configuration, a reference input is given to the system and the tracking response of the system is observed. The figure shows that the

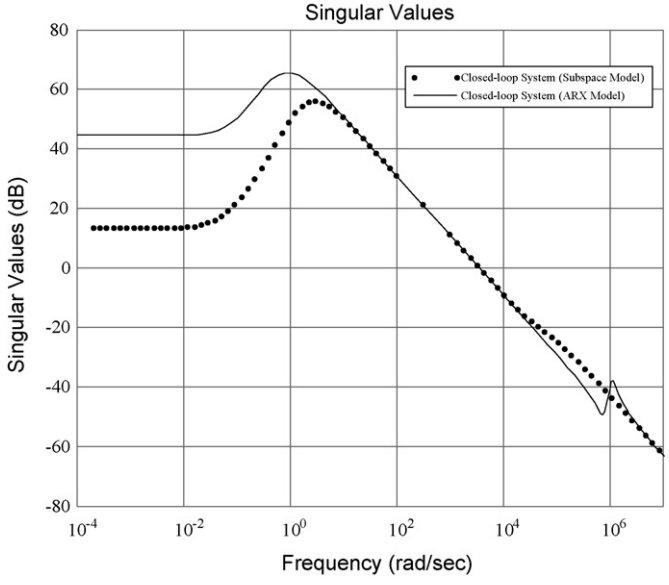

Fig. 6. Bode plot of complementary sensitivity functions (subspace and ARX models).

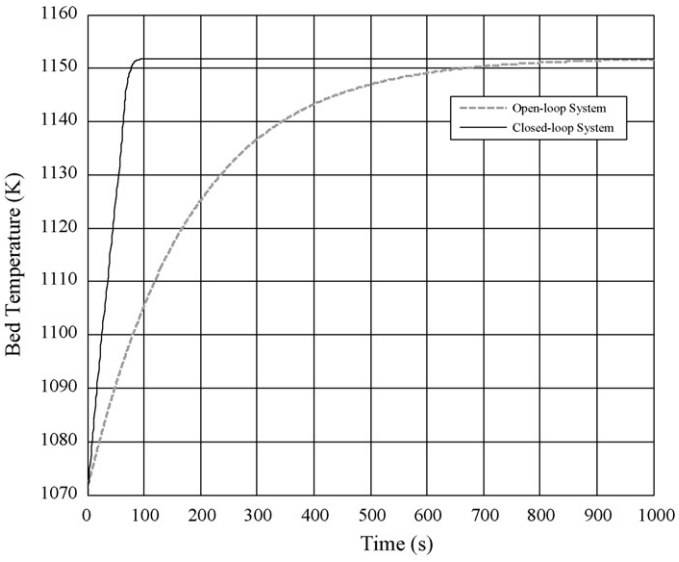

Fig. 7. Comparison between step responses of the closed-loop and open-loop systems.

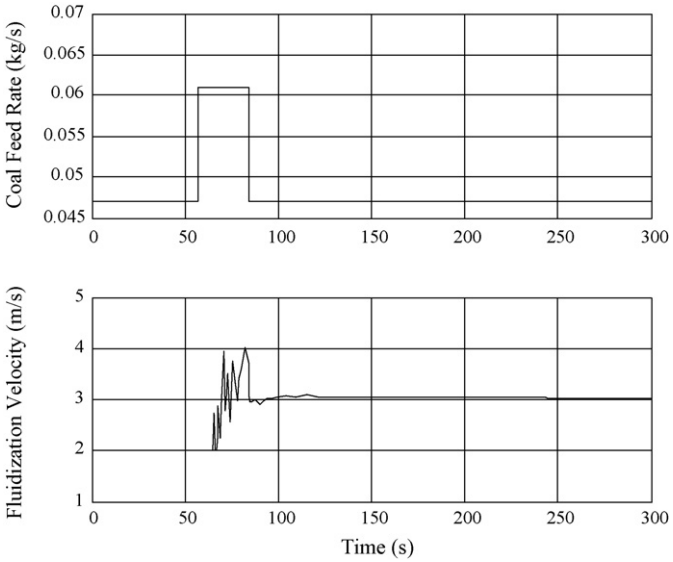

Fig. 9. The values of control inputs ($T_b = 1150$ K).

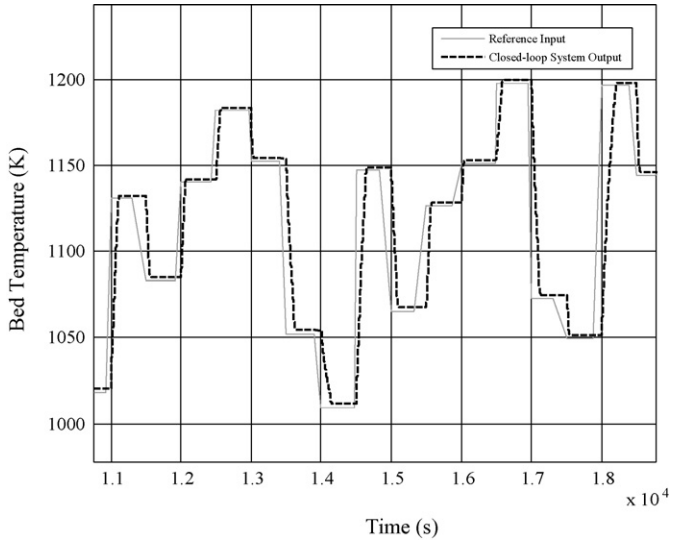

Fig. 8. System response to random level reference input.

controlled system satisfyingly tracks the input. As mentioned before, the operating bed temperature is usually in the range of 1100–1200 K but in the case of low-grade fuels the bed temperature can even be below 1070 K. The temperature ranges around 1120 K optimizing the sulfur capture efficiency of limestone, combustion efficiency, NO_x content and agglomeration of the bed material as well [15].

The inputs (coal feed rate and fluidization velocity) are bounded. It should be noted that to have an appropriate fluidization process, the fluidizing velocity must remain within a certain range. It should be bounded between the minimum fluidization velocity, u_{mf}, and the terminal velocity. Some of the problems concerning unbounded fluidizing velocity which results in improper solid circulation rate or suspension density are reduction in combustion efficiency and combustion chamber saturation and clinkering. The combustion efficiency generally decreases with increasing fluidizing velocity due to higher entrainment of the unburnt fines and oxygen bypassing. However, lower velocities may prevent fluidization and therefore run the risk of choking. If the velocity decreased further, the solid concentration in the column increases upto a point causing saturation of the column with the solids. The solids start accumulating, filling up the column and resulting in a steep rise in the pressure [2]. It is assumed that the coal feed rate is limited in the range 170–220 kg/h and the fluidization velocity is in the range 2–4.6 m/s. However, bounds on the control inputs were considered as one of the control objectives in our H_∞ design. If the system is forced to set the temperature to a desired value, the inputs must reach to a steady-state value when the control task is accomplished. For example in the case that our desired temperature is 1150 K and the inputs are bounded in the above-mentioned ranges, their final values reaches to 0.047 kg/s (170 kg/h) and 3.0 m/s for coal feed rate and fluidization velocity, respectively. Control inputs u_1 and u_2 in the case of 1150 K as the reference point are depicted in Fig. 9.

Maintenance of a stable inventory of solids is very important for the stable operation of a CFB boiler. This means that the total mass of solids in the bed must remain unchanged during the combustion process. Because it is too important to keep the bed inventory well-controlled so that it cannot become too high, causing the danger of high bed temperatures and sintering threat. The simulation results show that the total bed mass takes the steady-state value of 120 kg with a tolerance of ±10 kg, which is in the desired range.

A common robust stability test of any closed-loop is to see the effect of changes in system parameters on the system responses. As hinted before, change in the quality of the feed coal is one of the most challenging factors in modeling and control of CFB systems as it affects system dynamics. Coal particle diameter along with its volatile content and heat value change permanently during the combustion process and alter with the coal type. Also apparent activation energy for char particles of dif-

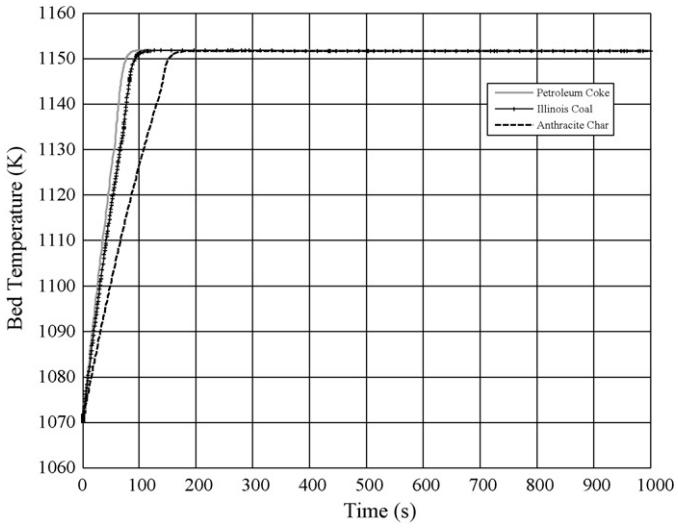

Fig. 10. System output to step reference input for different coal types.

ferent origins (from petroleum coke to brown coal) ranges from 67 kJ/mol to 142 kJ/mol.

The simulation results are shown for Illinois coal and anthracite char with different diameters, heat values, activation energy, char burning rate constants and attrition constants in Fig. 10. It is observed that change in the coal type does not affect the tracking output; however, for the anthracite char, the settling time of the system has been partly increased.

Note that the model and the designed controller are valid only within the area that the system is allowed to work (system operating points). It is always risky to use a model outside the area for which it has been validated.

6. Conclusion

Circulating fluidized beds exhibit very complex hydrodynamics caused by interactions between the gas and the solid phases. The motion of gases and solids are driven by mechanisms that are difficult to identify and describe. A novel mathematical model of bed temperature in a circulating fluidized bed combustor was proposed. The mathematical model obtained which is established on mass and energy conservation equations, lets us incorporate all the process dynamics in the model. Then the subspace method based on least squares estimation was used to extract a dynamical model of the bed temperature. The subspace method is found to be a good selection among other identification methods from the viewpoint of validity and complexity. Having uncertainties in the model structure, a robust control algorithm is necessary to control the bed temperature. These uncertainties are mostly changes in the fuel consumed (heat value, fuel particle size. . .) or caused by bed asymmetry. In this paper we gave a LMI solution to the H_∞ robust control of bed temperature system. The H_∞ controller minimizes the sensitivity of the closed-loop system to disturbances caused by dynamic and parametric uncertainties. Bed temperature control procedure is done via controlling the fluidization velocity and the coal feed rate. Combustion air controls are very important for burning conditions. More stable burning conditions allow a decrease in the excess air ratio, thus reducing nitrogen emissions and increasing thermal efficiency of the boiler. However, the air controls must also take into account the potential risk for the CO and hydrocarbon emissions if excess air is reduced to a very low level. The simulation results of the closed-loop system show the ability of the proposed controller to robustly control the bed temperature in the presence of uncertainties. The settling time is significantly decreased and the tracking error has been improved. Also it has been observed that the fuel inventory remains almost stable during the control process; the fuel inventory in the bed is one of the key variables in the combustion process, combustion rate, and formation of nitrogen and sulfur oxides. Finally, it was discussed that keeping the bed temperature in a certain range reduces the emission of gaseous pollutants and also improves the system overall efficiency while the sulfur capture is at its optimal level.

References

[1] S.N. Oka, Fluidized Bed Combustion, Marcel Dekker, Inc., New York, 2004.
[2] P. Basu, Combustion and Gasification in Fluidized Bed, CRC Press, 2006.
[3] J.G. Singer, Combustion: Fossil Power, Combustion Engineering, Inc., Windsor, Connecticut, 1991.
[4] G. Brem, Overall modeling of atmospheric fluidized bed combustion and experimental verification, in: M. Valk (Ed.), Atmospheric Fluidized Bed Coal Combustion, Elsevier Science B.V, Amsterdam, 1995.
[5] Y. Huang, R. Turton, J. Park, P. Famouri, E. Boyle, Dynamic model of the riser in circulating fluidized bed, Powder Technol. 163 (2006) 23–31.
[6] Y. Bolkan, F. Berruti, J. Zhu, B. Milne, Hydrodynamic modeling of CFB risers and downers, Int. J. Chem. React. Eng. 1 (2003) A51.
[7] A. Jalali, P. Famouri, J. Park, R. Turton, E. Boyle, H_∞ based state estimation on standpipe of a cold flow circulating fluidized bed, in: Proceedings of the IEEE International Conference on Systems, Man and Cybernetics, vol. 3, 2003, pp. 2320–2325.
[8] A. Davari, A. Patankar, P. Koduru, L.J. Shadle, L.O. Lawson, Modeling and Control of Circulating Fluidized Bed using Neural Networks, Annual Project Report, University/NETL Partnership Program http://www.netl.doe.gov/coal/gasification/projects/adv-gas/docs/NNmimo.pdf, 2001.
[9] H. Shim, P. Famouri, W.N. Sams, E.J. Boyle, A state estimation of the standpipe of a circulating fluidized bed using an extended Kalman filter, in: Proceedings of the 16th International Conference on Fluidized Bed Combustion, May, 2001, pp. 130–140.
[10] W.-C. Yang, A model for the dynamics of a circulating fluidized bed loop, in: P. Basu, J.F. Large (Eds.), Circulating Fluidized Bed Technology II, Pergamon Press, Oxford, 1988.
[11] D.J. Pallares, F. Johnsson, Fluid dynamic modeling of large CFB units, in: Proceedings of the 7th International Conference on Circulating Fluidized Beds (CFB7), Niagara Falls, Ontario, Canada, May, 2002, pp. 387–394.
[12] S.B. Pulluri, A. Davari, L. Shadle, Wavelet networks in online modeling of circulating fluidized bed, in: Proceedings of the Thirty-Seventh Southeastern Symposium on System Theory, Tuskegee, Alabama, March, 2005, pp. 216–220.
[13] A.A. Jalali, A. Hadavand, Bed temperature control of a circulating fluidized bed combustion system using H∞ algorithm, in: International Conference on Control, Automation and Systems, Seoul, Korea, 2007, pp. 2658–2662.
[14] A. Hadavand, H.R. Pourshaghaghi, A.A. Jalali, P. Famouri, Bed temperature control of a circulating fluidized bed combustion system, in: The 8th International Power Engineering Conference, Singapore, 2007, pp. 890–895.
[15] E. Karppanen, Advanced control of an industrial circulating fluidized bed boiler using fuzzy logic, Doctoral Dissertation, University of Oulu, Finland, 2000.

[16] D.-F. Wang, P. Han, N. Liu, Z. Dong, S.-M. Jiao, Modeling the circulating fluidized bed reactor using RBF-NN based on immune genetic algorithm, in: Proceedings of the IEEE 1st International Conference on Machine Learning and Cybernetics, Beijing, China, 2002.
[17] V. Manovic, M. Komatina, S. Oka, Modeling the temperature in coal char particle during fluidized bed combustion, Fuel, Corrected Proof (available online 11 June 2007), in press.
[18] A.D. Rychkov, K.P. Filipov, Numerical modeling of coal combustion processes in ecological clear circulating fluidized bed boiler units, in: Proceedings of the 4th Korea-Russia International Symposium on Science and Technology, KORUS, vol. 1, 2000, pp. 304–309.
[19] H. Cui, J. Chaouki, Effects of temperature on local two-phase flow structure in bubbling and turbulent fluidized beds of FCC particles, Chem. Eng. Sci. 59 (2004) 3413–3422.
[20] O. Levenspiel, Chemical Reactor Engineering, 3rd edition, John Wiley & Sons, New York, 1999.
[21] P. Basu, D. Subbarao, An experimental investigation of burning rate and mass transfer in a turbulent fluidized bed, Combust. Flame 66 (1986) 261–269.
[22] P. Basu, S.A. Fraser, Circulating Fluidized Bed Boilers: Design and Operations, Butterworth-Heinemann, 1991.
[23] M.L. De Souza-Santos, Solid Fuels Combustion and Gasification, Marcel Dekker, Inc., New York, 2004.
[24] J. Warnatz, U. Maas, R.W. Dibble, Combustion: Physical and Chemical Fundamentals, Modeling and Simulation, Experiments, Pollutant Formation, 4th edition, Springer-Verlag, Berlin, 2006.
[25] P. Basu, Combustion of coal in circulating fluidized-bed boilers: a review, Chem. Eng. Sci. 54 (1999) 5547–5557.
[26] M.A. Field, D.W. Gill, B.B. Morgan, P.G.W. Hawksley, Br. Coal Utiliz. Res. Assoc. Mon. Bull. 31 (6) (1967) 285–345.
[27] G. Donsi, L. Massimilla, M. Miccio, Carbon fines production and elutriation from the bed of a fluidized coal combustor, Combust. Flame 41 (1981) 57–64.
[28] P.K. Halder, Combustion of single coal particles in circulating fluidized bed, PhD Thesis, Technical University of Nova Scotia, 1989.
[29] E. Talmor, D. Benenati, Solids mixing and circulation in gas fluidized beds, AIChE J. 9 (1963) 536–540.
[30] W.-C. Yang, Fluidization, Solids Handling and Processing: Industrial Applications, Noyes Publications, New Jersey, 1998.
[31] Y. Courbariaux, Heat Transfer in a Circulating Fluidized Bed, Master of Science Thesis, University of New Brunswick, 1998.
[32] C.E. Baukal, Heat Transfer in Industrial Combustion, CRC Press, 2000.
[33] C.C. Werdmann, J. Werther, Solids flow pattern and heat transfer in an industrial scale fluidized bed heat exchanger, in: Proceedings of the 12th International Conference on Fluidized Bed Combustion, 2, 1993, pp. 985–990.
[34] R.J. Divilio, T.J. Boyd, Practical implications of the effect of solids suspension density on heat transfer in large-scale CFB boilers, Circulating Fluidized Bed Technol. IV (1993) 334–339.
[35] K.D. Kiang, K.T. Liu, H. Nack, J.H. Oxley, Heat transfer in fast fluidized beds, in: D.L. Kearns (Ed.), Fluidization Technology II, Hemisphere, Washington, DC, 1976, pp. 471–483.
[36] J.C. Chen, J.R. Grace, M.R. Golriz, Heat transfer in fluidized beds: design methods, Powder Technol. 150 (2005) 123–132.
[37] A. Dutta, P. Basu, Overall heat transfer to water walls and wing walls of commercial circulating fluidized bed boilers, J. I. Energy 75 (504) (2002) 85–90.
[38] EPA, AP 42, Stationary point and area sources. Chapter 1: External combustion sources Compilation of air pollutant emission factors, vol. I, 5th ed., 1998.
[39] H.J.A.F. Tulleken, Generalized binary noise test-signal concept for improved identification-experiment design, Automatica 26 (1) (1990) 37–49.
[40] Y. Zhu, Multivariable System Identification for Process Control, Elsevier Science, 2001.
[41] L. Ljung, System Identification: Theory for the User, 2nd edition, Prentice Hall, Inc., New Jersey, 1999.
[42] T. Katayama, Subspace Methods for System Identification, Springer-Verlag, London, 2005.
[43] B. Roffel, B. Betlem, Process Dynamics and Control: Modeling for Control and Prediction, John Wiley & Sons, Ltd., Chichester, West Sussex, 2006.
[44] L. Ljung, T. Glad, Modeling of Dynamic Systems, Prentice Hall, New Jersey, Inc., 1994.
[45] T. Asai, S. Hara, T. Iwasaki, Simultaneous parametric uncertainty modeling and robust control synthesis by LFT scaling, Automatica 36 (2000) 1457–1467.
[46] A. Dhawan, H. Kar, Optimal guaranteed cost control of 2D discrete uncertain systems: an LMI approach, Signal Process. 87 (12) (2007) 3075–3085.
[47] E.K. Boukas, Static output feedback control for stochastic hybrid systems: LMI approach, Automatica 42 (1) (2006) 183–188.
[48] B. Yao, F. Wang, LMI approach to reliable H_∞ control of linear systems, J. Syst. Eng. Electron. 17 (2) (2006) 381–386.
[49] H.-S. Ko, J. Jatskevich, G. Dumont, G.-G. Yoon, An advanced LMI-based-LQR design for voltage control of grid-connected wind farm, Electr. Pow. Syst. Res., Corrected Proof (available online 19 June 2007), in press.
[50] H. Xu, X. Liu, K.L. Teo, A LMI approach to stability analysis and synthesis of impulsive switched systems with time delays, Nonlinear Analysis: Hybrid Systems 2 (1) (2008) 38–50.
[51] S. Boyd, L.E. Ghaoui, E. Feron, V. Balakrishnan, Linear Matrix Inequalities in System and Control Theory, Society for Industrial and Applied Mathematics (SIAM), Philadelphia, 1994.
[52] C. Scherer, P. Gahinet, M. Chilali, Multiobjective output-feedback control via LMI optimization, IEEE T. Automat. Contr. 42 (7) (1997) 896–911.
[53] S.S.E.H. Elnashaie, P. Garhyan, Conservation Equations and Modeling of Chemical and Biochemical Processes, Marcel Dekker, Inc., New York, 2003.
[54] M. Chilali, P. Gahinet, H_∞ design with pole placement constraints: an LMI approach, IEEE T. Automat. Contr. 41 (1996) 358–367.